C3 peptide enhances recovery from spinal cord injury by improved regenerative growth of descending fiber tracts

Francesco Boato[1,*], Sven Hendrix[1,2,*], Stefanie C. Huelsenbeck[3], Fred Hofmann[3], Gisela Große[4], Susann Djalali[4], Lars Klimaschewski[5], Maria Auer[5], Ingo Just[3], Gudrun Ahnert-Hilger[4,*] and Markus Höltje[4,*,‡]

[1]Center for Anatomy, Institute of Cell Biology and Neurobiology, Charité-Universitätsmedizin Berlin, Charitéplatz 1, D-10117 Berlin, Germany
[2]Department of Morphology and BIOMED Institute, Hasselt University, Agoralaangebouw A, B-3590 Diepenbeek, Belgium
[3]Institute of Toxicology, Hannover Medical School (MHH), Carl-Neuberg-Straße 1, D-30625 Hannover, Germany
[4]Center for Anatomy, Functional Cell Biology, Charité-Universitätsmedizin Berlin, Charitéplatz 1, D-10117 Berlin, Germany
[5]Division of Neuroanatomy, Department of Anatomy, Histology and Embryology, Innsbruck Medical University, Müllerstraße 59, A-6020 Innsbruck, Austria

*These authors contributed equally to this work
‡Author for correspondence (markus.hoeltje@charite.de)

Accepted 2 March 2010
Journal of Cell Science 123, 1652-1662

doi:10.1242/jcs.066050

Summary

Functional recovery and regeneration of corticospinal tract (CST) fibers following spinal cord injury by compression or dorsal hemisection in mice was monitored after application of the enzyme-deficient *Clostridium botulinum* C3-protein-derived 29-amino-acid fragment C3bot$^{154-182}$. This peptide significantly improved locomotor restoration in both injury models as assessed by the open-field Basso Mouse Scale for locomotion test and Rotarod treadmill experiments. These data were supported by tracing studies showing an enhanced regenerative growth of CST fibers in treated animals as visualized by anterograde tracing. Additionally, C3bot$^{154-182}$ stimulated regenerative growth of raphespinal fibers and improved serotonergic input to lumbar α-motoneurons. These in vivo data were confirmed by in vitro data, showing an enhanced axon outgrowth of α-motoneurons and hippocampal neurons cultivated on normal or growth-inhibitory substrates after application of C3bot$^{154-182}$. The observed effects were probably caused by a non-enzymatic downregulation of active RhoA by the C3 peptide as indicated by pull-down experiments. By contrast, C3bot$^{154-182}$ did not induce neurite outgrowth in primary cultures of dorsal root ganglion cells. In conclusion, C3bot$^{154-182}$ represents a novel, promising tool to foster axonal protection and/or repair, as well as functional recovery after traumatic CNS injury.

Key words: CNS injury, Nerve growth, Neuroregeneration, Raphespinal tract, Basso Mouse Scale

Introduction

Since their discovery over 20 years ago bacterial C3 transferases have been used to study the function of Rho proteins in virtually all cellular systems of eukaryotic origin (Aktories and Just, 2005; Vogelsgesang et al., 2007). C3-family proteins have been proven to foster neurite outgrowth and regeneration in a variety of in vitro and in vivo systems (Jin and Strittmatter, 1997; Lehmann et al., 1999; Fischer et al., 2004; Bertrand et al., 2005; Bertrand et al., 2007). Thus, their application represents one interventional strategy for stimulating intrinsically limited neuronal regeneration following injury to the central nervous system (CNS). Rodent spinal cord injury (SCI) is an established model for investigating putative beneficial effects of various forms of intervention, and C3 proteins were successfully used to improve functional recovery after SCI in rats and mice (Dergham et al., 2002; Lord-Fontaine et al., 2008). Its mode of action, namely enzymatic inactivation of Rho proteins (especially RhoA in the context of cytoskeletal rearrangements), which serve as neuronal growth inhibitors, is well understood and has been known for a long time. Non-enzymatic interactions and cellular effects were also recently discovered. For example, application of enzyme-deficient C3 protein from *C. botulinum* to primary cultures of hippocampal neurons resulted in a significant stimulation of axon outgrowth (Ahnert-Hilger et al., 2004). Building on these findings we were able to show that the biologically active region of clostridial C3 protein (C3bot) responsible for non-enzymatic action is localized within a region comprising the amino acids 154-182 (Höltje et al., 2009). Treatment of primary neuronal cultures with this 29-amino-acid fragment resulted in increased axonal and dendritic growth accompanied by a higher number of synaptic contacts. Moreover, application of C3bot$^{154-182}$ promoted fiber outgrowth and reinnervation of target tissues in organotypical hippocampal/entorhinal slice cultures (Höltje et al., 2009). Thus, it became clear that C3bot also exerts its growth-promoting effects on neurons by an enzyme-independent activity. However, effects on glial cells such as astrocytes or microglia are strictly dependent on enzymatic Rho inactivation (Höltje et al., 2008; Hoffmann et al., 2008), which demonstrates specificity of enzyme-independent effects on neurons.

In the current study, we investigated the ability of C3bot$^{154-182}$ to stimulate central axonal repair by anterograde tracing followed by histochemical analysis, as well as by functional analysis of recovery after contusive SCI or spinal dorsal hemisection. Restoration of motor function was monitored by the Basso Mouse Scale for locomotion (BMS) (Basso et al., 1995; Basso et al., 2006) and the Rotarod treadmill (Sheng et al., 2004). Potential effects on regenerative axonal outgrowth within the spinal cord in response to treatment with C3bot$^{154-182}$ were analyzed by anterograde tracing of the corticospinal tract (CST) with

biotinylated dextran amine. Investigations of spinal fiber outgrowth also included an analysis of descending brainstem fibers, such as serotonergic raphespinal projections, including their projections onto lumbar motoneurons. Furthermore, we addressed the question whether C3bot$^{154-182}$ affects the maintenance of neuromuscular junctions of tibial skeletal muscles following SCI. Additionally, putative C3bot$^{154-182}$-mediated effects on neurite morphology and active RhoA levels of certain subsets of cultivated neurons relevant to the in vivo data were investigated.

Results

We first investigated the in vivo effects of the 29-amino-acid fragment C3bot$^{154-182}$ on functional recovery after contusion injury or dorsal hemisection of the spinal cord in mice (Figs 1, 2). Gel foam patches soaked in C3bot$^{154-182}$ solution (40 µM, 610 ng per animal) were applied directly above the injury site (see also Fig. 3A). We analyzed the locomotor function in these mice using the BMS – an open-field test (Fig. 1) – and a Rotarod treadmill to analyze the performance under forced movement (Fig. 2). In the BMS analysis, the locomotor function was significantly increased during the whole observation period in contusion-injured mice treated with C3bot$^{154-182}$ patches (Fig. 1A). The motor performance of both treated and untreated mice was more affected in the hemisection model than after contusion injury. The clear beneficial effect of the C3 peptide in the former model was particularly pronounced during the last 2 weeks of the observation period (Fig. 1B). Here, the observation period was extended to 4 weeks (compared with 3 weeks in the contusion model) because the lesion was more severe. Since correct foot placing is associated with correct CST function (De Ryck et al., 1992; Metz and Whishaw, 2002), we also analyzed stepping and correct paw positioning scores for the contusion model (Fig. 1C). Treated animals showed improved stepping and, especially, paw positioning from day 8 onwards and with substantial improvement over subsequent days, whereas control animals had minimal scores throughout the observation period (Fig. 1C,D). Both the BMS and the stepping and paw positioning tests were performed in two separate independent experiments with consistent results.

Furthermore, C3bot$^{154-182}$ application increased the latency for the mice to fall from the Rotarod in both models (Fig. 2A,B). However, the positive effects were more consistent following contusion injury than after hemisection. Detailed photodocumentation (Fig. 2C, shown for the contusion injury model) revealed that treated mice displayed more efficient climbing behavior on the turning wheel, whereas control mice showed a tendency to lose grip early, at low rotation speed. After completing the behavioral examination we addressed whether the improved recovery of treated animals included enhanced axonal growth of descending spinal motor fibers. Analysis of the BDA-traced CST showed a significantly increased percentage of nerve fibers between

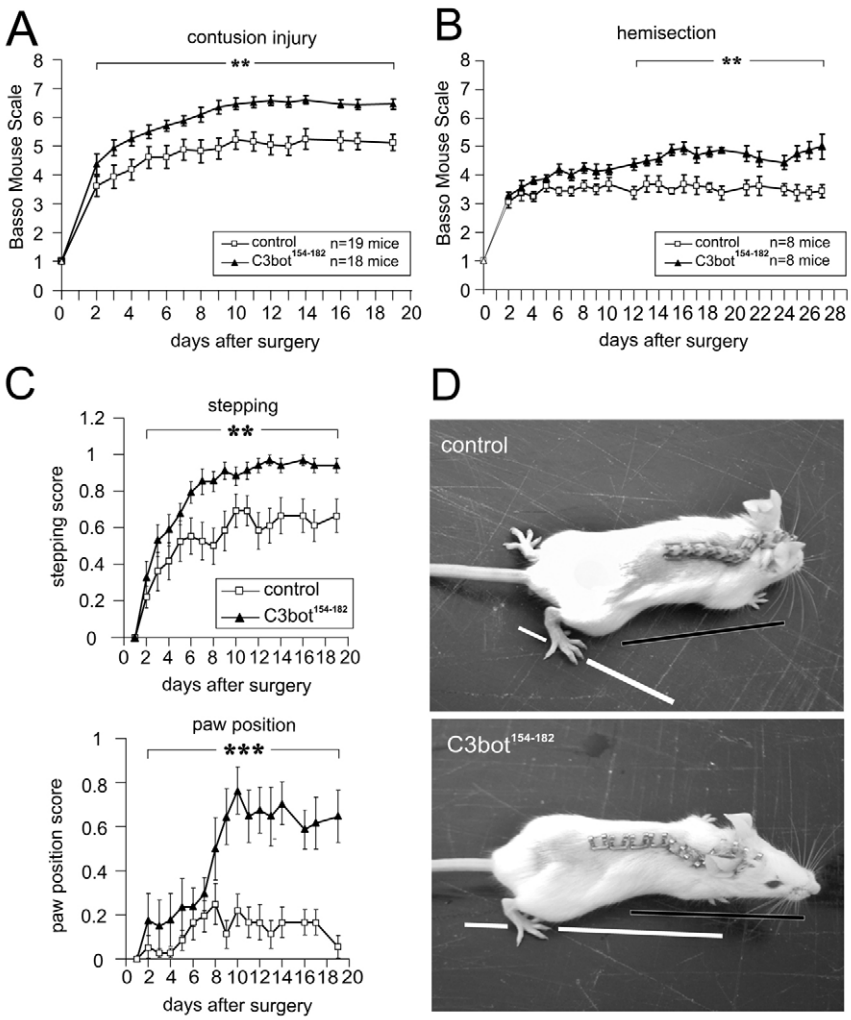

Fig. 1. Local C3bot$^{154-182}$ application improves the clinical outcome after spinal cord injury in mice in an open field test. (**A**) C3bot$^{154-182}$ application (5 µl or 40 µM) significantly increased the performance after contusion SCI more than 1 scale point according to the BMS. (**B**) Application of C3bot$^{154-182}$ also improved the functional recovery of mice following dorsal hemisection of the spinal cord. (**C**) Stepping performance and correct positioning of the paw were analyzed for the contusion SCI. Both parameters were found to be significantly improved following treatment with C3bot$^{154-182}$. (**D**) Representative photo documentation of improved stepping performance and correct positioning of the paw in treated contusion-injured mice. The black line indicates the body axis, whereas the white line represents the orientation of the middle finger of the right hind paw, indicating substantial rotation in control mice and parallel orientation after C3bot$^{154-182}$ application. $^{**}P<0.01$ and $^{***}P<0.001$.

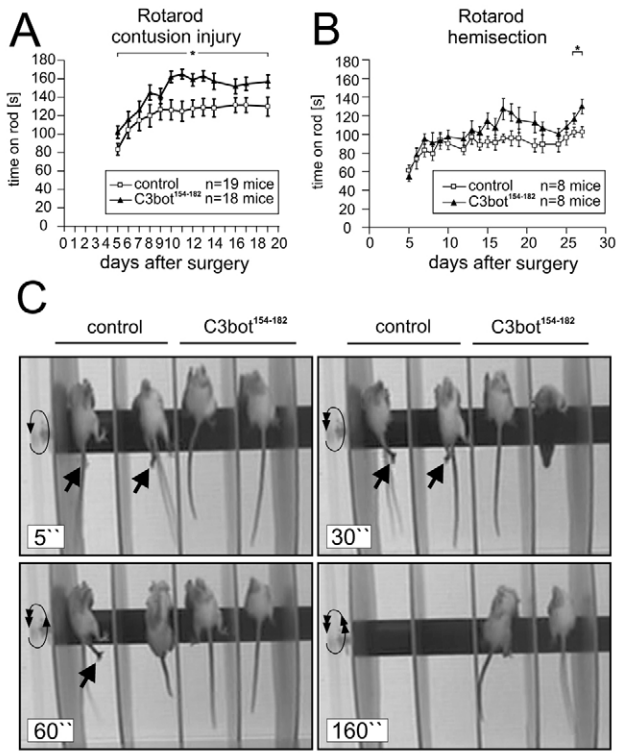

Fig. 2. Local C3bot$^{154-182}$ application improves locomotor performance during forced movement after SCI in mice. (**A**) C3bot$^{154-182}$ application (5 µl or 40 µM) significantly increased the latency time until contusion-injured mice jumped off the Rotarod. (**B**) Treatment with C3bot$^{154-182}$ following dorsal hemisection also resulted in an improved performance. The effect was less pronounced than that observed after contusion injury. (**C**) Representative photo documentation of improved locomotor function after C3bot$^{154-182}$ application to contusion-injured mice. The arrows indicate paws of two control mice losing grip of the turning wheel at early time points, whereas the two treated mice on the right side climb on the wheel efficiently. After 160 seconds the control mice had already jumped off the wheels, whereas the treated mice continued to perform well. The increasing speed of rotation is indicated by the number of arrowheads on the circular arrow. *P<0.05.

the end of the tract and the center of the contusion injury lesion. Moreover, the number of fibers passing through the lesion center was significantly increased at 0.5 mm (Fig. 3, Fig. 4A-C). In line with the latter, an increased number of BDA-positive fibers caudal to the lesion site was detected following hemisection and treatment with the C3 peptide (Fig. 4D-F). We even detected an increased percentage of regenerating nerve fibers as far as 5 mm caudal from the lesion center (Fig. 4F). Taken together, the data at this stage provided strong evidence of a C3bot$^{154-182}$-mediated improvement of axonal sprouting and/or regeneration following damage to the spinal cord. Additionally, the early onset of improvement, especially in the BMS tests following contusion injury, indicated that the C3 peptide also has neuroprotective effects.

To detect possible effects of C3bot$^{154-182}$ on the lesion size and reactive gliosis, spinal cord sections were double-stained for glial acidic fibrillary protein (GFAP) and myelin basic protein (MBP). Evaluation of contusion-induced lesion size revealed a reduction of tissue damage by 25% following administration of C3 peptide (Fig. 5A-C). However, gliosis as measured by perilesional GFAP expression by reactive astrocytes was not significantly altered by C3bot$^{154-182}$ (Fig. 5D). In the hemisection model, neither lesion size nor astrogliosis were affected by the peptide (supplementary material Fig. S1). However, recovery of function after SCI might not exclusively rely on regenerative growth of CST fibers. To test for beneficial effects of C3 peptide on other tracts beside the CST we visualized serotonergic raphespinal projections by an anti-serotonin (5HT) antiserum in mice injured by hemisection (Fig. 6A-E). In the ventral funiculus the total length of serotonergic fibers was assessed cranial and caudal to the lesion site (Fig. 6A,B). Whereas the total fiber length cranial to the lesion was unaltered after application of C3bot$^{154-182}$, it was significantly increased caudal to the lesion at more than three-fold compared with control mice (Fig. 6C,D). Serotonergic fibers set up a network of projections to the grey matter in order to contact interneurons and motoneurons. Previous research suggested that serotonergic fibers originating from the brainstem form conventional synapses with theses neurons within the ventral horn (Rajaofetra et al., 1992). It is well established that serotonergic input to spinal motoneurons activates motor functions (Jacobs et al., 2002). Consequently, we addressed the question whether treatment with C3 peptide leads to an increased serotonergic input to lumbar motoneurons and whether this contributes to the improved motor outcome. At lumbar levels L1-L2 we counted 5HT-positive boutons on α-motoneurons of the ventral horn. We found that application of C3bot$^{154-182}$ considerably increased the average number of serotonergic contacts from 3.6 (per 100 µm cell perimeter) to 10.3 (Fig. 6F,G). Notably, the increased serotonergic contacts corresponded very well to the increased density of serotonergic fibers within the ventral funiculus caudal to the lesion site. Taken together, these data provide strong evidence for a C3-peptide-mediated improved serotonergic input to lumbar α-motoneurons, thereby contributing to an enhanced hind-limb motor performance.

In addition to the investigations described above, we studied the putative effects of C3bot$^{154-182}$ treatment on the neuromuscular junctions of tibial muscles of the hind limb (*M. tibialis cranialis*) following injury at the end of the observation period. The tibial muscles are crucially involved in lifting the paw during movement on both level surfaces and when clinging to a (rotating) rod. After longitudinal sectioning, we applied the established labeling technique using Alexa-Fluor-488-coupled α-bungarotoxin (Guntinas-Lichius et al., 2005) to visualize and quantify motor endplates (Fig. 7A,B). Following contusion, the number of motor endplates decreased by 17% (normalized to the number of muscle fibers) in the control-SCI group compared with intact mice. This reduction in the number of motor endplates was completely prevented following administration of C3bot$^{154-182}$ (Fig. 7C). After hemisection, loss of endplates in general was more severe. The number of endplates in the PBS group was declined to 55% (Fig. 7C). Treatment with the C3 peptide restored the number of endplates to 85%. No obvious differences in the size or general morphology of endplates were detected between the groups.

We next addressed whether C3bot$^{154-182}$ directly influences axon outgrowth of α-motoneurons. To this end, we prepared dissociation cultures of the spinal cord. To establish a situation more like that of the in vivo CNS lesion, we cultivated the cells on growth-inhibitory substrates, such as chondroitin sulfate proteoglycans (CSPG), which are widely known to reduce neurite outgrowth. To identify cultured α-motoneurons we used size criteria and detected non-phosphorylated neurofilament protein H by SMI-32 staining (Bar-Peled et al., 1999). To examine putative C3bot-peptide effects, spinal cord cultures were incubated with 50 nM of C3bot$^{154-182}$.

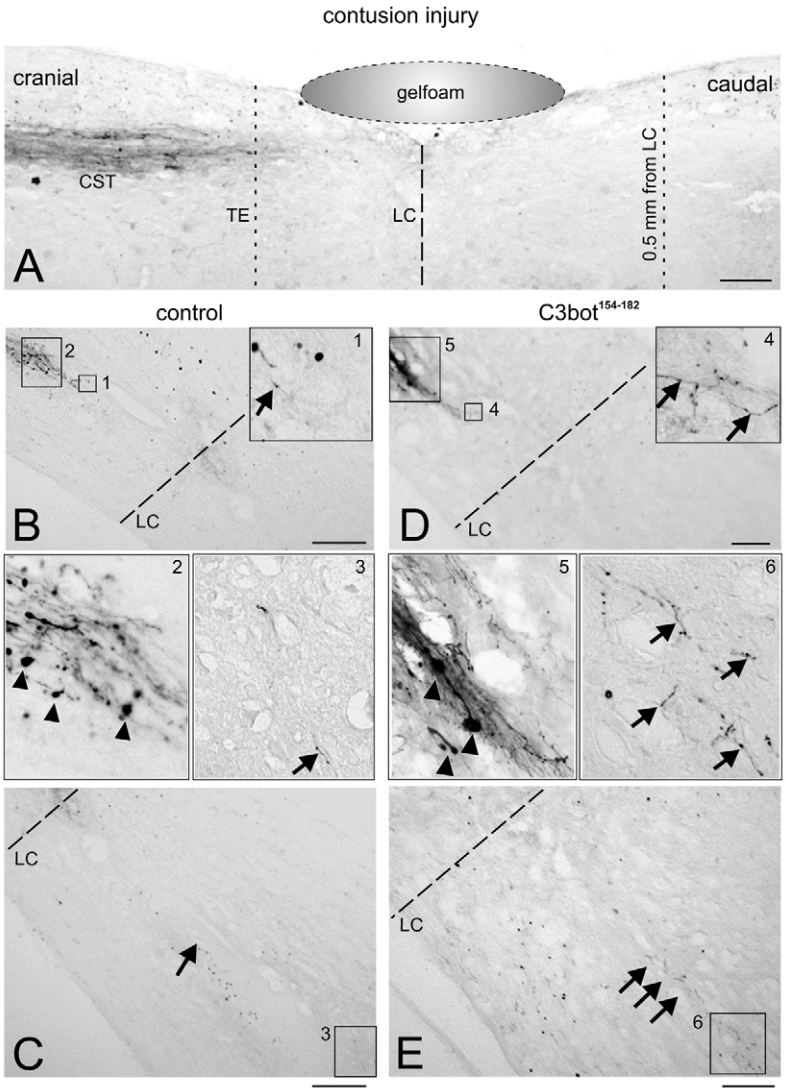

Fig. 3. Local C3bot$^{154-182}$ application increases the number of CST nerve fibers between the tract end and the lesion site, and caudal to the lesion after spinal cord compression injury in mice. (**A**) Representative micrograph illustrating the application of a gel foam patch soaked in C3bot$^{154-182}$ solution on top of the lesion at thoracic segment T8. CST, corticospinal tract; LC, lesion center; TE, end of corticospinal tract. (**B-E**) Representative micrographs of the area between tract end and lesion center (B,D) and distal of the lesion center (C,E). Numbered and boxed areas indicate higher magnification images. Arrowheads indicate retraction bulbs; arrows indicate nerve fibers between the tract end and the lesion site, and between fibers passing through the lesion center. Inserts 1 and 3 in PBS-treated control mice compared with inserts 4 and 6 show increased numbers of nerve fibers in mice after C3bot$^{154-182}$ application. Scale bars: 100 μm.

Morphometrical analysis revealed that C3bot$^{154-182}$ application to α-motoneurons increased axon length by 25% on normal substrate (Fig. 8A,B). Axon outgrowth on inhibitory CSPG substrate without C3bot$^{154-182}$ was reduced by ~50%. Addition of the C3 peptide completely prevented the growth-inhibiting effect of the CSPG coat (Fig. 8B). Under either condition α-motoneurons had no tendency to develop extensive axonal branching and in many cases total axonal length reflected the length of a single non-branched axonal process. Next, we addressed whether C3bot$^{154-182}$ also reduced the growth-inhibiting effects of CSPG on other neuron populations such as hippocampal neurons, thus, representing a general principle. Primary hippocampal cultures were cultivated on either poly-L-lysine alone or CSPG-coated coverslips. Cells were double-stained against neurofilament (NFP) or microtubule-associated protein 2 (Map2) to mark axons or dendrites, respectively (Fig. 8C,D). Incubation with C3bot$^{154-182}$ significantly promoted axonal length and branching as well as dendrite length on both normal and inhibitory substrates. As demonstrated for α-motoneurons, the addition of the C3 peptide completely abolished the growth-inhibitory effect by CSPG (Fig. 8D).

We next investigated whether the beneficial influence on axonal outgrowth was specific for central neurons or extended to peripheral neurons. We used primary cultures of adult rat dorsal root ganglion cells to check for alterations in axonal morphology after application of C3bot$^{154-182}$. None of the parameters analyzed (total and maximal axon length, as well as axonal branching) was significantly altered by the C3 peptide (supplementary material Fig. S2). By contrast, incubation with full-length enzyme-competent C3bot positively influenced all of the parameters investigated.

To gain insight into the molecular mechanisms contributing to the observed morphological changes we determined active RhoA levels by rhotekin pull-down analysis from hippocampal cell lysates. RhoA is known to be crucially involved in actin and microtubule dynamics. Application of C3bot$^{154-182}$ at final concentrations of 10 nM or 30 nM to hippocampus cultures resulted in a strong reduction of active RhoA levels, whereas total RhoA protein expression was unchanged (Fig. 9). Thus, despite the lack of enzymatic activity, the C3 peptide is likely to exert its effects by means of a RhoA-dependent mechanism.

Discussion

In this study, we demonstrate that a 29-amino-acid fragment derived from full-length *C. botulinum* C3 protein (C3bot) improves recovery from spinal cord injury. In previous studies, we have

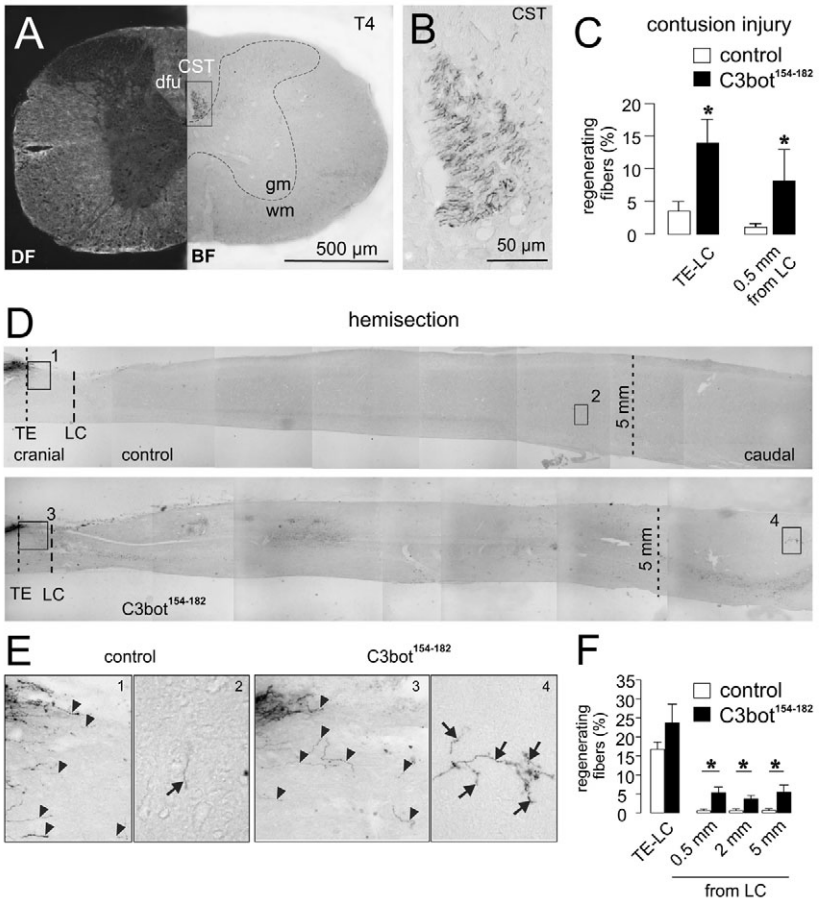

Fig. 4. Quantification of BDA-labeled nerve fibers between the tract end and the lesion site and that cross the lesion in two models of spinal cord injury in mice: promoting effects of C3bot$^{154-182}$. (**A**) Cross section of spinal cord at thoracic level 4 (T4) illustrating correct tracing of the left CST with the majority of fibers in the dorsal funiculus. The dashed line indicates the boundary between grey and white matter. BF, brightfield illumination; DF, darkfield illumination; dfu, dorsal funiculus; gm, gray matter; wm, white matter. (**B**) Enlargement of the boxed area in A depicting the dorsal corticospinal tract (CST). (**C**) The percentage of labeled nerve fibers was significantly increased in contusion-injured mice treated with C3bot$^{154-182}$ compared with controls. Here, the number of labeled fibers at the T4 level proximal to the lesion was calculated within a standardized area. Bars represent the percentage of nerve fibers in the area between the end of the CST and the lesion center (TE-LC) and in the area 0.5 mm distal to the lesion center (0.5 mm from LC). PBS, n=6 animals; C3bot$^{154-182}$, n=5 animals. (**D**) Parasaggital spinal cord sections of mice that underwent SCI by dorsal hemisection. Images show CST tracing. TE, tract end; LC, lesion center. (**E**) Higher magnification of the numbered and boxed areas in D. Arrowheads indicate nerve fibers between the tract end and the lesion site, arrows indicate fibers passing the lesion center. (**F**) The percentage of labeled nerve fibers caudal to the lesion was significantly increased in hemisection-injured mice treated with C3bot$^{154-182}$ compared with control mice. Bars indicate the percentage of nerve fibers in the area between the end of the CST and the lesion center (TE-LC) and in the area 0.5 mm, 2 mm and 5 mm distal to the lesion center. PBS, n=5 animals; C3bot$^{154-182}$, n=7 animals. *P<0.05.

shown that C3bot function is not restricted to its enzymatic mode of action (Ahnert-Hilger et al., 2004; Höltje et al., 2009). There, we detected promoting effects on axon and dendrite outgrowth mediated by enzyme-deficient full-length C3 protein and by C3bot$^{154-182}$ in several in vitro systems. Our current study now clearly shows that treatment with C3bot$^{154-182}$ is also effective in vivo.

Behavioral analysis

We studied two spinal-cord-injury models. Although the most common type of SCI in humans involves compressive impact (Sekhon and Fehlings, 2001), cutting CST fibers by performing a hemisection up to at least the central canal creates a more-defined lesion and allows distinguishing between newly formed – and, therefore, regenerated – and spared fibers (Sicotte et al., 2003; Steward et al., 2003). Two experimental settings that were designed to observe functional recovery after spinal cord injury detected an improved motor performance in treated animals as early as within the first week following compression injury. This early onset of improved functional recovery might indicate not only beneficial effects on neurological repair mechanisms but also a neuroprotective effect of C3bot$^{154-182}$. This evidence was underlined by the fact that treatment with the peptide resulted in reduced tissue damage (lesion size) following contusive SCI. The compression-induced injury (1 second of pressure with 20 cN) approximates the rapid force and/or acceleration injuries common to weight-drop-models, thus, an ischemic component is not probable but cannot be fully excluded.

The lesion size was unaltered after dorsal hemisection and the beneficial effects of the peptide appeared later than using the contusion-injury model. In the latter, the BMS score demonstrated significant benefit only 2 days post-injury, and this positive trend persisted throughout the almost 3-week observation period. Upon completion, treated animals exhibited a higher degree of coordination between fore limbs and the affected hind limbs (Basso et al., 2006). Additionally, improved locomotor restoration, such as frequent plantar stepping and parallel paw position relative to the body axis, contributed to the improved outcome. Both plantar stepping and especially paw positioning showed the highest improvement following C3bot$^{154-182}$ treatment during the final 2 weeks of the observation period. Furthermore, the BMS open-field data were well supported by the Rotarod forced-movement experiments and emphasized the effectiveness of the treatment. Hemisection represented a more-severe injury in general (according to the BMS scores and the Rotarod experiments, both control and treated animals performed worse than after contusion injury). Nevertheless, in both tests the effect of the C3 peptide was observed, particularly in the final days of the observation period.

Histological analysis of the spinal cord

To determine whether the improved functional recovery after SCI was reflected by histological differences between the different treatment groups, we first quantified BDA+ axons of the CST. In animals treated with C3bot$^{154-182}$ a significantly enhanced number of BDA-labeled axons caudal to the lesion site were observed following both contusion injury and hemisection. Increased

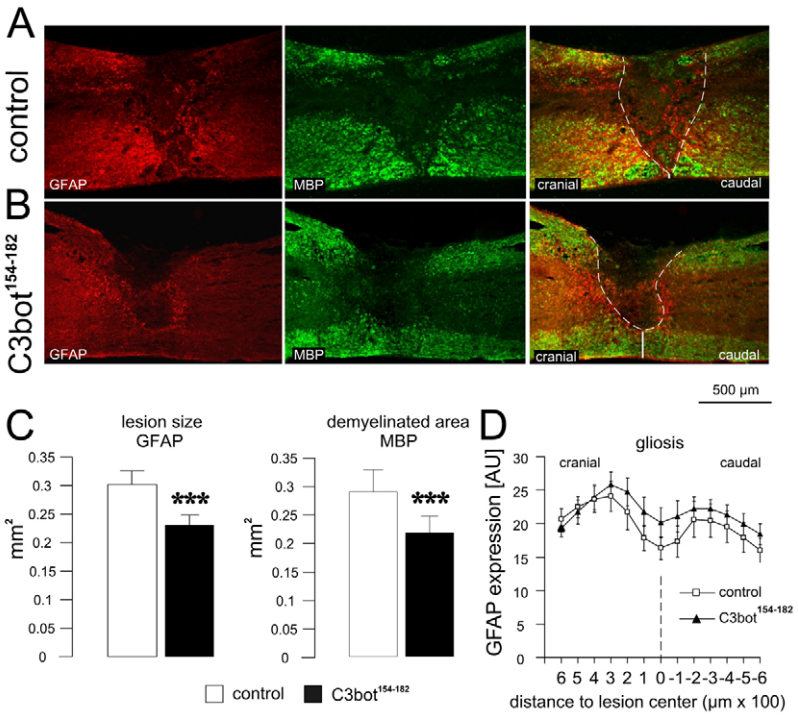

Fig. 5. C3bot$^{154-182}$ reduces the lesion size after contusive SCI. (**A**,**B**) Micrographs of parasaggital spinal cord sections including the contusion injury site. Sections were double-stained for expression of glial fibrillary acidic protein (GFAP) and myelin basic protein (MBP) to evaluate the lesion size. Tissue damage was reduced in animals treated with C3bot$^{154-182}$. The dashed line outlines the area of the lesion. Vertical bars indicate spared tissue at the lesion center. (**C**) Quantification of the lesion size according to the perilesional astrocytes and demyelinated area. Both measurements indicated a reduction of the lesion size by around 25% after application of C3bot$^{154-182}$. (**D**) Quantification of GFAP expression from 600 µm cranial to 600 µm caudal to the lesion center demonstrated no significant difference in astrocytic reactions between control and treated animals. PBS, n=5 animals; C3bot$^{154-182}$, n=5 animals. ***P<0.001.

numbers of fibers cranial to the lesion were also observed in the case of contusion. Indicators such as distance or time course of growth can also be employed to characterize axonal response in terms of plasticity, sprouting or regeneration (Cafferty et al., 2008). Particularly in the hemisection model, we detected alterations in axonal growth over moderate distances (<1 mm from the end of the CST) – which might indicate local regenerative sprouting, but also over a distance as far as 5 mm from the lesion center – which is likely to represent regeneration. We can exclude that the fibers detected caudal to the lesion originated from uninjured ventral CST fibers, because in our hemisection model the ventral funiculus was severed by a median cut in addition to the transection of the dorsal half of the spinal cord. Even though the data provide a static view of the axonal growth situation at a defined time point, we can assume that the enhanced number of fibers detected mainly after compression injury between the retraction bulb and the lesion center are a mixture of newly grown and spared axons protected by the application of C3bot$^{154-182}$. Interestingly, local growth of lesioned fibers cranial to the site of injury seems to contribute to faster recovery from SCI such that synaptic connections are established to propriospinal neurons (Bareyre et al., 2004). In line with this, we have shown previously that C3bot$^{154-182}$ enhances the formation of synaptic connections in vitro (Höltje et al., 2009). On the basis of morphological criteria, the BDA+ fibers crossing the lesion site appear to represent newly established fibers, even though in the compression-injury model we cannot exclude that they represent branching from spared fibers. Supporting our CST data, enhanced numbers of serotonergic fibers caudal to the lesion were observed in mice treated with C3bot$^{154-182}$ following hemisection. Moreover, serotonergic input to lumbar α-motoneurons of the ventral horn was enhanced to a similar degree by the peptide. In the mammalian spinal cord, the predominant role of 5HT, which mainly originates from medullary raphe nuclei, seems to be the facilitation of motor performance as well as the coordination between motor, autonomic and sensory systems (Skagerberg and Björklund, 1985; Allen and Cechetto, 1994; Kim et al., 2004; Boido et al., 2009). Our findings of improved serotonergic input to lumbar motoneurons, thus, provide strong evidence for one probable mechanism that leads to enhanced functional recovery in mice treated with C3bot$^{154-182}$. However, a mixture of axonal responses, including those of local circuits – for example at lumbar spinal cord segments harboring the hind limb α-motoneurons – might have additionally contributed to the observed improved clinical outcome.

Motor-endplate counts

Animals treated with C3bot$^{154-182}$ exhibited a reduced motor-endplate loss in a tibial muscle (*M. tibialis cranialis*) following both lesion types. Following hemisection, the number of motor endplates was more strongly reduced than after contusion of the spinal cord. This observation correlates with the behavioral data, showing lower locomotory scores and shorter times on the treadmill for mice injured by hemisection. In general, several factors might contribute to the loss of neuromuscular junctions after SCI. These could include the lack of use and subsequent muscle atrophy. As known from studies in rat, denervation of tibial muscles can result in a remarkable reduction of motor-endplate counts (of up to 90%) without further treatment (Iwata et al., 2006). In our spinal-cord-injury models the hind-limb muscles were not denervated by peripheral nerve lesion but experienced reduced activation by activity-deprived motoneurons. Mice treated with C3 peptide exhibited increased serotonergic input to α-motoneurons together with increased motor activity and, therefore, the deleterious effects might have been largely prevented. Furthermore, direct protective and/or growth-promoting effects on α-motoneurons elicited by C3bot$^{154-182}$ cannot be ruled out because the treatment of cultivated α-motoneurons effectively promoted axon growth, especially when cultivated on inhibitory substrates.

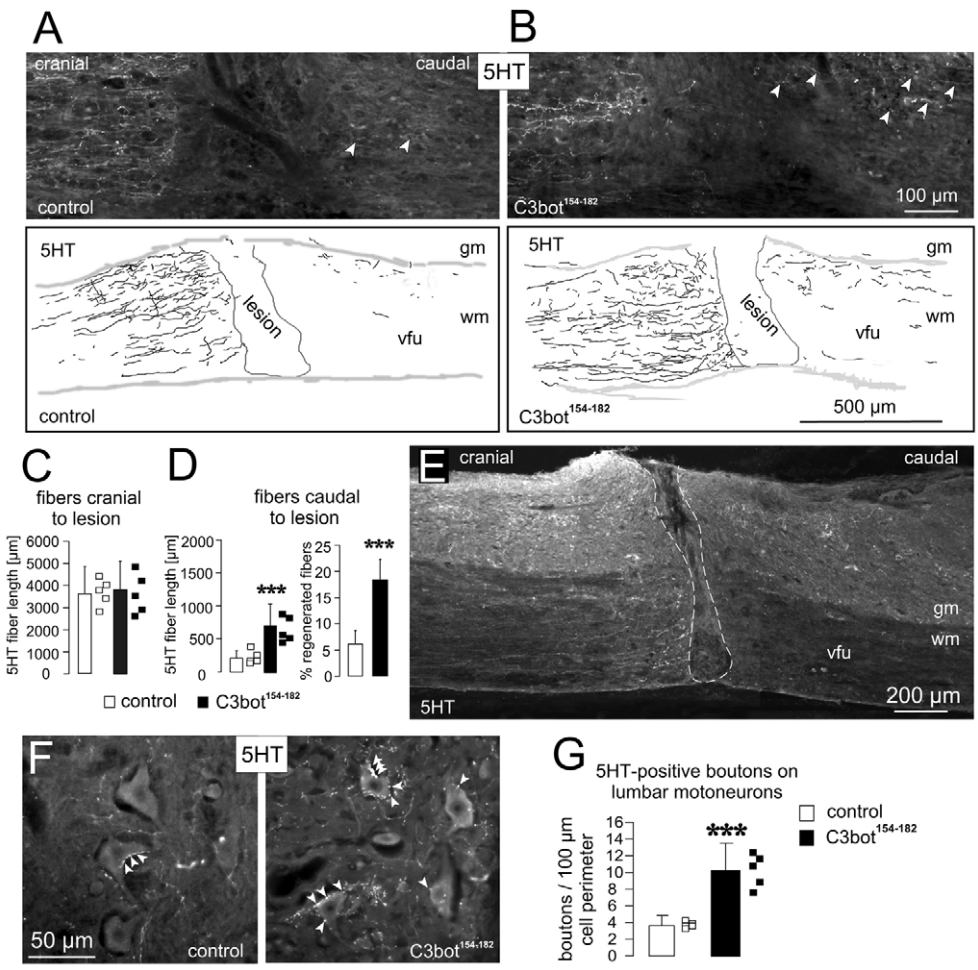

Fig. 6. C3bot$^{154-182}$ increases raphespinal axon outgrowth and serotonergic input to lumbar α-motoneurons after SCI by hemisection. (**A**,**B**) Images taken from the ventral funiculus at the lesion site of animals that received either PBS (A) or C3bot$^{154-182}$ (B). Arrowheads indicate serotonergic fibers caudal to the lesion. Neurolucida-style drawing (superimposed images of three sections) of serotonergic fibers from two animals (one per condition) showing an increased fiber growth caudal to the lesion in the treated animals. (**C**) Analysis of total fiber length within the ventral funiculus cranial to the lesion. Five animals per condition were analyzed. Squares represent mean values of individual animals. Pooled data showed no difference between groups. (**D**) Analysis of total fiber length within the ventral funiculus caudal to the lesion (left panel) indicates a significant increase in fiber length of treated animals. The percentage of regenerated fiber length was calculated from these data (right panel). Application of C3bot$^{154-182}$ increased the percentage three-fold. (**E**) Parasaggital section giving an overview of spinal cord from mice lesioned by hemisection SCI and stained with a serotonin (5HT) antibody. Note that, in addition to the dorsal spinal cord, the ventral funiculus is transected in this lesion model by a cut along the midline. The dashed line indicates the area of the lesion. gm, gray matter; wm, white matter; vfu, ventral funiculus. (**F**) Representative micrographs that show α-motoneurons of the ventral horn at lumbar level L2. Arrowheads depict 5HT-positive boutons contacting the cell bodies. (**G**) Quantification of 5HT-positive boutons on motoneurons relative to the cell body perimeter. Treatment with C3bot$^{154-182}$ increased the number of serotonergic terminals almost three-fold. ***P <0.001.

The use of C3bot$^{154-182}$ to treat spinal cord injuries

Numerous studies have demonstrated that clostridial C3 proteins foster axonal repair mechanisms after traumatic injury to the CNS. Inhibiting the small GTPase Rho as a master negative regulator of axonal growth (Niederost et al., 2002; Schweigreiter et al., 2004) improved regeneration in both rat and mice SCI models (for a review, see Ruff et al., 2008). Inhibition of Rho was achieved by both the direct enzymatical inactivation through C3 transferases (Dergham et al., 2002; Dubreuil et al., 2003) and the pharmacological inhibition of p160ROCK-mediated downstream signaling (Fournier et al., 2003). However, increasing evidence indicates that C3 transferases also act through mechanisms other than an enzymatic Rho inactivation. Some years ago C3 proteins were shown to bind to the small GTPase RalA, thereby inactivating Ral signaling, which is involved in a variety of cellular functions (Wilde et al., 2002; Pautsch et al., 2005). Additionally, pioneering studies by our group showed that the application of enzyme-deficient full-length C3bot or fragments of it elicits growth-promoting effects on cultivated neurons (Ahnert-Hilger et al., 2004; Höltje et al., 2009). The pull-down studies presented here provide the first evidence of the molecular mechanisms of C3bot$^{154-182}$ action. Our data clearly show that C3bot$^{154-182}$ can reduce levels of active RhoA by an as-yet-unknown non-enzymatic mechanism. Possibilities include the one that RhoA is influenced directly by the internalized peptide or indirectly through inhibition of GEF (guanine nucleotide exchange factors) or activation of GAP

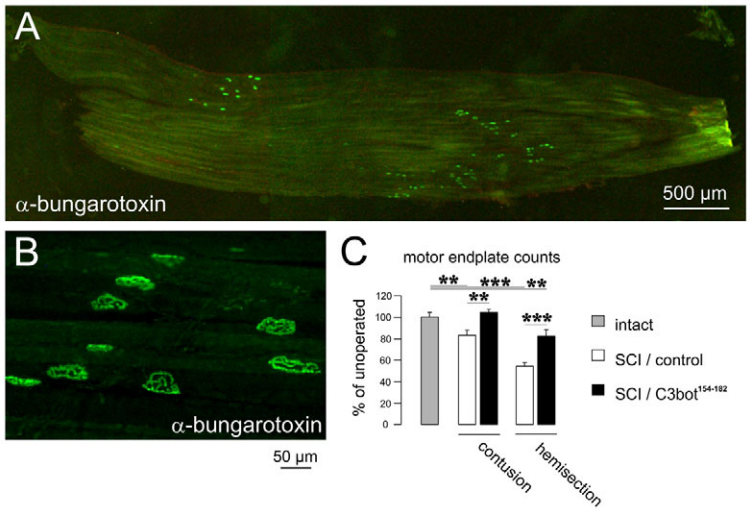

Fig. 7. C3bot$^{154-182}$ reduces motor endplate loss after SCI. *Tibialis cranialis* muscles from intact and lesioned mice were dissected from both hind limbs of transcardially perfused animals. Motor endplates were stained with Alexa-Fluor-488-conjugated α-bungarotoxin. (**A**) Sample picture (contusion-lesioned, PBS) of a longitudinal muscle section at low-power magnification. Staining for α-bungarotoxin shows the distribution of motor endplates that appear as green spots. (**B**) Staining of a group of endplates at higher magnification. (**C**) Quantification of motor endplates. The number of motor endplates and muscle fibers per section were quantified. Counts were obtained from individual sections of either intact (set as 100%) or lesioned PBS- or C3bot$^{154-182}$-treated animals (three animals per group). Data show that C3bot$^{154-182}$ reduced motor endplate loss both after contusion injury and hemisection of the spinal cord. Intact, *n*=38. Contusion injury: PBS, *n*=78 sections; C3bot$^{154-182}$, *n*=64 sections. Hemisection: PBS, *n*=57 sections; C3bot$^{154-182}$ *n*=57 sections. ***P*<0.01 and ****P*<0.001.

(GTPase activating proteins). Inactivation of neuronal RhoA by C3bot$^{154-182}$ signaling could well explain our observation that the growth-inhibitory effect of chondroitin sulfate proteoglycans (CSPG) from reactive astrocytes (Fuller et al., 2007) – which is mediated by Rho activation (Jain et al., 2004; Schweigreiter et al., 2004) – is largely prevented in vitro. In summary, our data indicate a direct, neuron-specific effect because no enzyme-independent effects were observed on glial cells in response to C3 preparations

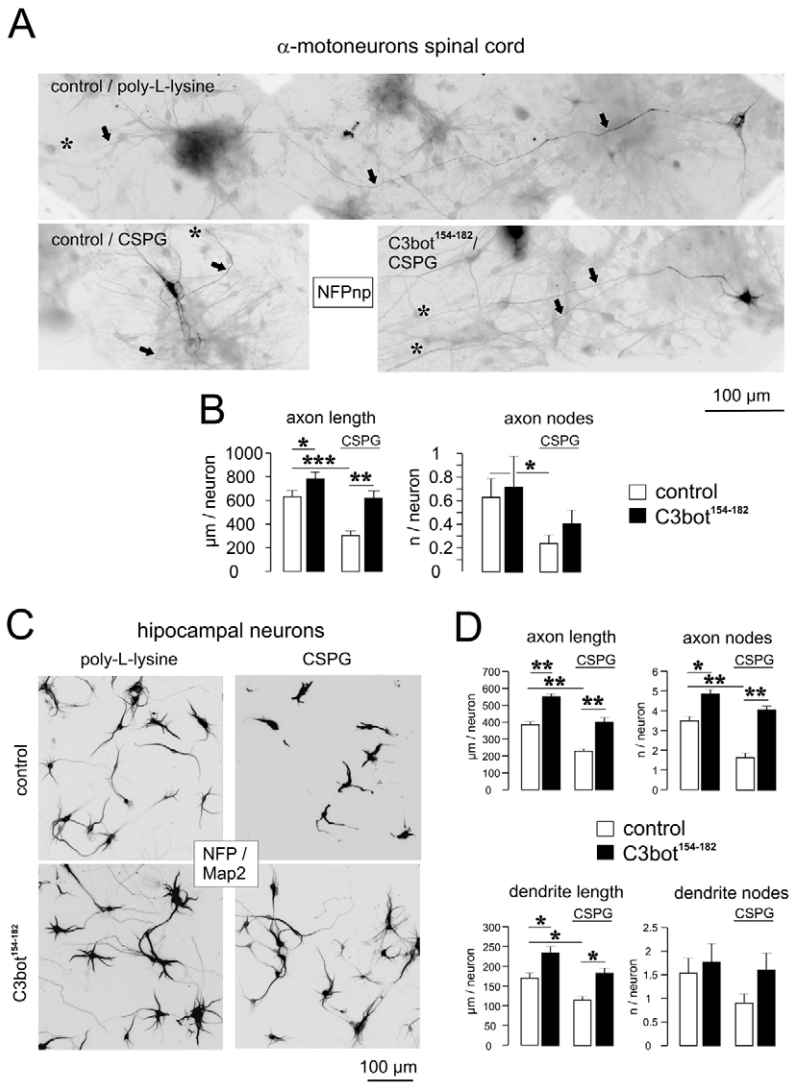

Fig. 8. C3bot$^{154-182}$ enhances axon outgrowth of α-motoneurons and hippocampal neurons. (**A**) Micrographs of embryonic spinal cord cultures cultivated on normal poly-L-lysine coating or on a mix of growth-inhibitory chondroitin sulfate proteoglycans (CSPG). Neurons were incubated with or without the addition of C3bot$^{154-182}$. Large neurons expressing non-phosphorylated neurofilament H (NFPnp) could be identified as α-motoneurons. (**B**) Morphometrical analysis of the effects of C3bot$^{154-182}$. Incubation of cultures for four days with the C3 peptide (50 nM) resulted in a significant increase in axon length of cultivated α-motoneurons on normal coating. Cultivation on CSPG substrate strongly reduced axonal length. Note that application of C3bot$^{154-182}$ completely prevented the growth-inhibitory effect of CSPG. Axonal branching was poorly developed under either condition (see scale). Diagrams represent data from 30 neurons per condition from five independent experiments. (**C**) Photomicrographs of embryonic hippocampus neurons cultivated on normal or CSPG substrate as described above. Neurons were double-stained for NFP and microtubule associated protein 2 (Map2) to mark axons and dendrites, respectively (images show the combined staining to illustrate the complete cell morphology). (**D**) Morphometrical analysis of the effects of C3bot$^{154-182}$. Incubation of cultures for four days with the C3 peptide (50 nM) resulted in a significant increase in axon length and branching, as well as dendrite length on normal coating. Cultivation on CSPG substrate strongly reduced these parameters. Again, application of C3bot$^{154-182}$ completely prevented the growth-inhibitory effect of CSPG. Diagrams represent data from 40 neurons per condition from two independent experiments. **P*<0.05, ***P*<0.01 and ****P*<0.001.

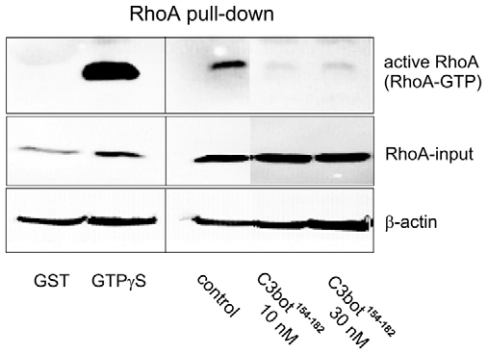

Fig. 9. Inhibition of active RhoA by C3bot$^{154-182}$. Hippocampal neurons were treated for 4 days with 10 nM or 30 nM of C3bot$^{154-182}$. Active RhoA levels were determined from cell lysates by Rho-binding rhotekin pull-down assay. Incubation with both concentrations of C3bot$^{154-182}$ for 48 hours resulted in a strong inhibition of Rho activity, as demonstrated by the reduction of GTP-bound RhoA. Controls using glutathione-bound GST only, as well as addition of non-hydrolyzable unlabeled GTP (GTPγS) to untreated cultures confirmed correct assay function. β-Actin levels served as internal standard.

(Höltje et al., 2005; Höltje et al., 2008; Hoffmann et al., 2008). The clear specificity of effects makes this peptide an excellent candidate for fostering the growth of neuronal processes without eliciting potentially unwanted glia-derived side effects. The failure of C3bot$^{154-182}$ to promote axon growth of cultivated DRG neurons indicates that specific receptor equipment is necessary that is only present in central neurons (because all in vitro effects observed so far were obtained at doses as low as in the nanomolar range).

Taken together, these data indicate that the short C3bot-derived amino-acid fragment C3bot$^{154-182}$ is a new and promising tool to specifically enhance process outgrowth of central neurons and promote recovery after traumatic injury to the CNS.

Materials and Methods

Generation of the C3bot-derived peptide

C3bot$^{154-182}$ was synthesized at IPF PharmaCeuticals GmbH (Hannover, Germany). The lyophilized peptide was reconstituted in PBS pH 7.5, sterile filtered (0.22 μm) and used for the experiments as indicated. C3bot was expressed as recombinant GST-fusion protein in *E. coli* TG1 harboring the respective DNA fragment in the plasmid pGEX-2T (Höltje et al., 2009).

Spinal cord surgeries and CST tracing

Contusion injury

Spinal cord compression injury, CST tracing and analysis was performed as described previously (Sieber-Blum et al., 2006). Briefly, 9- to 11-week-old anesthetized Balb/C mice (20-24 g) underwent a partial laminectomy at thoracic level T8, and a contusion lesion was performed with a SPI Correx Tension/Compression Gage (Penn Tool, Maplewood, NJ) modified for precise compression of the mouse spinal cord at 20 cN for 1 second, thus, this injury type approximates the rapid force/acceleration injuries common to weight drop models. After positioning of the gelfoam patch on top of the perforated dura, the muscles were sutured and the back skin closed with wound clips. A small hole was then drilled into the skull and a Hamilton syringe was inserted into the motor cortex to apply 2 μl biotinylated dextran amine (10% BDA) which is known to be transported anterogradely. BDA$^+$ CST nerve fibers were visualized by DAB staining. BDA$^+$ CST nerve fibers cranial and caudal to the lesion were counted in serial sections and normalized to the number of labeled fibers within a standardized 20-μm-wide area across the mid-dorsoventral diameter of the CST in cross sections at the T4 level cranial to the lesion. Representative documentation of the CST at the T4 level is shown in Fig. 4A,B.

Dorsal hemisection

For the spinal cord bilateral dorsal hemisection, iridectomy scissors were used to transect left and right dorsal funiculus, the dorsal horns (Simonen et al., 2003) and, additionally, the ventral funiculus, resulting in a complete transection of the dorsomedial and ventral CST. Following this procedure, mice were treated as described above.

Locomotion tests

Mice were continuously tested for functional recovery within 3 or 4 weeks (contusion injury or hemisection, respectively) following SCI with the Basso Mouse Scale (BMS) (Basso et al., 2006). The BMS is a ten-point locomotor rating scale (ranging from 9=normal locomotion to 0=complete hind-limb paralysis), in which mice are scored by two investigators who were unaware of the experimental groups based on hind-limb movements made in an open field during a 4-minute interval. Since correct foot placing correlates with proper CST function (De Ryck et al., 1992; Metz and Whishaw, 2002) and because subscores for each attribute of the BMS can be used to reveal recovery responses for individual locomotor features (Basso et al., 2006), stepping performance and correct paw positioning were evaluated. The scoring of the stepping was performed to emphasize whether plantar stepping was present in less (score of 0) or more (score of 1) than 50% of the steps, provided the animal was moving at least three body lengths at consistent speed. These parameters are not covered by the classical BMS subscore. Analysis of paw positioning, provided the plantar stepping was frequent or consistent, was performed by determining whether the paws were rotated both at initial contact (IC) and lift off (LO) (paw-positioning score 0), parallel at IC but rotated at LO (paw-positioning score 1) or parallel both at IC and LO (paw-positioning score 2).

After allowing the mice to recover for 5 days, Rotarod performance (Sheng et al., 2004) was determined continuously until the end of the observation periods. The mice were placed on an accelerated rolling rod (Ugo Basile, Comeris, VA, Italy). The latency to jump off from the rod was automatically recorded by the action of the mouse dropping onto a trigger plate.

Histological analysis of labeled CST nerve fibers

To trace regenerative growth of the CST, biotinylated dextran-amine (BDA) was injected into the right motor cortex and visualized by DAB staining on perfusion-fixed cryosections of the spinal cord. BDA-labeled nerve fibers of the CST were quantified between the track end and the lesion, as well as at defined distances caudal to the lesion (Sieber-Blum et al., 2006). Fibers were counted on five to seven adjacent sections per animal. Using strict criteria [outlined in Steward et al. (Steward et al., 2003)] all sections were carefully analyzed to exclude the presence of unlesioned fibers.

Histological analysis of spinal cord tissue

Lesion size and fiber analysis

Spinal cord cryosections (20 μm) obtained 3 weeks (contusion) or 3 weeks (hemisection) after surgery from animals that had been transcardially perfused with 4% formaldehyde were preincubated with 10% normal goat serum dissolved in PBS containing 0.5% Triton X-100 for 30 minutes at room temperature (RT). Incubation with primary antibodies was carried out overnight at 4°C. Following repeated washing steps with PBS, secondary antibodies were applied for 2 hours at RT. After removal of unbound antibodies, sections were mounted. For measurement of lesion size and gliosis, 5-6 sections per animal (five animals per group) containing the lesion center were analyzed. Lesion size was evaluated by double-staining against glial fibrillary acidic protein (GFAP) and myelin basic protein (MBP) using mouse monoclonal and rabbit polyclonal antibodies, respectively, both from Chemicon International (Hofheim, Germany). Alexa Fluor 594 horse anti-mouse and Alexa Fluor 488 goat anti-rabbit antibodies (Molecular Probes, Eugene, OR) were used as secondary antibodies. Quantification of GFAP expression was performed through intensity analysis using Adobe Photoshop software (San Jose, CA) within rectangular areas of 100 μm (width) × dorsoventral diameter of spinal cord (height) extending from 600 μm cranial to 600 μm caudal from the lesion center (Wang et al., 2009).

For analysis of serotonergic fibers and 5HT-positive boutons on lumbar α-motoneurons spinal cord sections were incubated with a polyclonal anti 5-HT antiserum obtained from Immunostar (Hudson, WI). Alexa Fluor 488 goat anti-rabbit (Molecular Probes) was used as secondary antibody. 5-HT-expressing fibers were documented and analysed in the ventral funiculus extending from 600 μm cranial to 600 μm caudal of the lesion center (area size 600×400 μm). Total length of serotonergic fibers was calculated using Image J open source software (NIH). Fiber analysis was performed from three to four parasaggital sections per animal. For camera lucida tracing, Adobe Photoshop software was used.

Quantification of 5HT-positive boutons on lumbar α-motoneurons

α-motorneurons of lumbar segments 1 to 2 (L1-L2) of the most ventral part of the ventral horn (representing Rexed's lamina 9) were analyzed. The number of 5HT-positive boutons on motoneurons was calculated according to the criteria given elsewhere (Müllner et al., 2008). Briefly, 5HT-positive swellings directly contacting α-motoneuron somata were counted in relation to the cell-body perimeter as measured by Leica Application Suite software (Leica Microsystems, Wetzlar, Germany). Measurements are expressed as number of boutons per 100 μm cell perimeter. Per animal (n=5 for each group), between 22 and 24 neurons were analyzed.

Analysis of motor endplates

The *M. tibialis cranialis* was dissected from both hind limbs of transcardially perfusion-fixed animals. Muscles were postfixed with 1% formalin for 1 hour and cryoprotected overnight in 20% sucrose at 4°C. Muscles were cut in 30-μm longitudinal sections on a cryostat. For staining oft the motor endplate, sections were

incubated for 2 hours at RT with 2 μg/ml Alexa-Fluor-488-conjugated α-bungarotoxin (Molecular Probes). Every second section was analyzed and the total number of motor endplates per individual section was determined. Additionally, muscle fibers across the mid-belly diameter of the muscle were counted for each section and motor-endplate counts were normalized to the number of discernible muscle fibers.

Primary culture of α-motoneurons

Cells were prepared from cervical and thoracic spinal cord segments of embryonic day 13 (E13) mice and treated as above. One day after plating of cells at a density of 1×10^5 cells per well, C3bot peptide was added to the culture medium. Four days later, i.e. at 5 days in vitro (DIV5) neurons were fixed with 4% formaldehyde for 15 minutes and then permeabilized for 30 minutes at RT using 0.3% Triton X-100 dissolved in PBS. Motoneurons were stained by a monoclonal antibody against neurofilament H non-phosphorylated protein (SMI-32, Hiss Diagnostics, Freiburg, Germany) overnight at 4°C. After washing in PBS, secondary antibodies were applied for 1 hour at RT. Approximately 15-30 cells per coverslip were stained using this procedure. For morphometrical analysis only the largest cells with diameters between 30 and 50 μm, presumably representing α-motoneurons, were considered for measurements.

Primary culture of hippocampal neurons

Cells were prepared from fetal mice at embryonic day 16 (E16). Dissected pieces of hippocampi were rinsed first with PBS, then with dissociation medium (MEM, supplemented with 10% fetal calf serum, 100 IE insulin/l, 0.5 mM glutamine, 100 U/ml penicillin/streptomycin, 44 mM glucose and 10 mM HEPES buffer) and then dissociated mechanically. Following centrifugation, cells were resuspended in starter medium (serum-free neurobasal medium supplemented with B27, 0.5 mM glutamine, 100 U/ml penicillin/streptomycin and 25 μM glutamate) and plated at a density of 1×10^4 cells per well on glass coverslips pre-coated with poly-L-lysine/collagen. For incubation on inhibitory substrate, an additional coating with 10 μg/ml chondroitin sulfate proteoglycans (Proteoglycan Mix, Millipore, Billerica, MA) was performed. All other ingredients were obtained from Gibco/BRL Life Technologies, Eggenstein, Germany. One day after plating C3bot$^{154-182}$ was added to the culture medium. Four days later (DIV5) neurons were fixed. Neurons were stained by using a monoclonal antibody against neurofilament protein (NFP, 200 kDa) or a polyclonal antiserum against microtubule associated proteins 2 (MAP2), both from Chemicon International, to label axons or dendrites, respectively.

Primary culture of dorsal root ganglion cells

Dorsal root ganglia obtained from adult rats (200-250 g) were treated with collagenase (5000 units/ml) for 60 minutes in RPMI medium. After another 15 minutes in 0.25% trypsin/EDTA they were transferred to RPMI medium containing 10% horse serum and 5% fetal bovine serum, followed by 5-15 passages through a fire-polished Pasteur pipette. Defined medium (RPMI containing N2 supplements and antibiotics) was added and neurons were plated at a density of 200-300 per glass floor dish (Willco Wells B.V., Amsterdam, NL; 3.8 cm^2 area/dish) coated overnight with 0.1 mg/ml poly-D-lysine and 20 μg/ml laminin for 4 hours. One hour after seeding, the medium was carefully changed to remove cellular debris and C3bot preparations were added. Cultures were maintained for 1 day at 37°C in a humidified atmosphere under 5% CO_2 in the presence of antimitotic agents. Neurons were then fixed for 10 minutes with 4% formaldehyde. After two washes in PBS and permeabilization with 0.5% Triton X-100, the cells were incubated in 0.3% bovine serum albumin (in PBS) for 5 minutes. Primary monoclonal antibodies raised against the 200-kDa neurofilament protein (Sigma-Aldrich, Deisenhofen, Germany) were applied for 2 hours and detected by anti-mouse secondary antibodies conjugated to Cy3 purchased from Dianova (Hamburg, Germany).

Morphometrical analysis

Dissociated α-motoneurons and hippocampal neurons were documented using a Leica DMLB microscope equipped with a DFC 490 digital camera, and were morphometrically analyzed using Neurolucida software (MicroBrightField, Williston, VT) to determine total axonal length and overall number of branches. The parameter 'axon length' represents the integral length of all visible parts of an axon, including its higher order branches. Dorsal root ganglion cells were documented using an inverted fluorescence microscope (Zeiss Axiovert 100) equipped with a SPOT RT digital camera. Metamorph software (Molecular Devices, Sunnyvale, CA) was applied to measure total axon length, the longest of all vectors from the centroid of the cell body to the growth cones (maximal distance) and the number of axonal branch points per neuron. All morphologically intact neurons per dish with axons longer than the cell diameter were analyzed.

Rho GTPase pull-down assay

The Rho-binding domain C21 (kind gift of John Collard, The Netherlands Cancer Institute, Amsterdam, The Netherlands), encoding the N-terminal 90 amino acids of human rhotekin, was expressed as GST fusion protein in *E. coli* and purified by affinity chromatography using glutathione-sepharose. Hippocampal neurons were lysed in lysis buffer (50 mM Tris, pH 7.2; 150 mM NaCl; 5 mM $MgCl_2$; 1% Nonidet P-40; 1 mM phenylmethanesulfonyl fluoride; 5 mM dithiothreitol; and protease inhibitor cocktail, EDTA-free). The obtained suspension was subsequently sonicated on ice. The soluble fraction was obtained by centrifugation (10,000 ***g*** for 10 minutes). Lysates were then added to glutathione-bound GST-C21 (rhotekin) for 1 hour (4°C). The beads were washed three times, and bound proteins were mobilized by incubation with Laemmli sample buffer at 95°C for 10 minutes. Samples were subjected to SDS-PAGE and western blot analysis.

Statistical analysis

Data represent mean values ± s.e.m. Locomotion tests were analyzed using a two-way ANOVA. Statistical significance of cytochemical data was tested using the Mann Whitney U test.

The authors are indebted to Birgit Metze, Annemarie Löchner and Julia König for their engaged and skillful technical assistance, and Ari Liebkowsky for editing the text. Work was supported by a grant from the Deutsche Forschungsgemeinschaft (DFG) to G.A.H. and I.J., and the Fonds zur Förderung der wissenschaftlichen Forschung (FWF) to L.K. This study was also supported in part by grants from the Berlin-Brandenburg Center for Regenerative Therapies and the University of Hasselt to S.H. (BOF09NI07). F.B. is a fellow of the Marie Curie EST CORTEX network.

Supplementary material available online at
http://jcs.biologists.org/cgi/content/full/123/10/1652/DC1

References

Ahnert-Hilger, G., Höltje, M., Grosse, G., Pickert, G., Mucke, C., Nixdorf-Bergweiler, B., Boquet, P., Hofmann, F. and Just, I. (2004). Differential effects of Rho GTPases on axonal and dendritic development in hippocampal neurones. *J. Neurochem.* **90**, 9-18.

Aktories, K. and Just, I. (2005). Clostridial Rho-inhibiting protein toxins. *Curr. Top. Microbiol. Immunol.* **291**, 113-145.

Allen, G. V. and Cechetto, D. F. (1994). Serotoninergic and nonserotoninergic neurons in the medullary raphe system have axon collateral projections to autonomic and somatic cell groups in the medulla and spinal cord. *J. Comp. Neurol.* **350**, 357-366.

Bareyre, F. M., Kerschensteiner, M., Raineteau, O., Mettenleiter, T. C., Weinmann, O. and Schwab, M. E. (2004). The injured spinal cord spontaneously forms a new intraspinal circuit in adult rats. *Nat. Neurosci.* **7**, 269-277.

Bar-Peled, O., Knudson, M., Korsmeyer, S. J. and Rothstein, J. D. (1999). Motor neuron degeneration is attenuated in bax-deficient neurons in vitro. *J. Neurosci. Res.* **55**, 542-556.

Basso, D. M., Beattie, M. S. and Bresnahan, J. C. (1995). A sensitive and reliable locomotor rating scale for open field testing in rats. *J. Neurotrauma* **12**, 1-21.

Basso, D. M., Fisher, L. C., Anderson, A. J., Jakeman, L. B., McTigue, D. M. and Popovich, P. G. (2006). Basso Mouse Scale for locomotion detects differences in recovery after spinal cord injury in five common mouse strains. *J. Neurotrauma* **23**, 635-659.

Bertrand, J., Winton, M. J., Rodriguez-Hernandez, N., Campenot, R. B. and McKerracher, L. (2005). Application of Rho antagonist to neuronal cell bodies promotes neurite growth in compartmented cultures and regeneration of retinal ganglion cell axons in the optic nerve of adult rats. *J. Neurosci.* **25**, 1113-1121.

Bertrand, J., Di Polo, A. and McKerracher, L. (2007). Enhanced survival and regeneration of axotomized retinal neurons by repeated delivery of cell-permeable C3-like Rho antagonists. *Neurobiol. Dis.* **25**, 65-72.

Boido, M., Rupa, R., Garbossa, D., Fontanella, M., Ducati, A. and Vercelli, A. (2009). Embryonic and adult stem cells promote raphespinal axon outgrowth and improve functional outcome following spinal hemisection in mice. *Eur. J. Neurosci.* **30**, 833-846.

Cafferty, W. B., McGee, A. W. and Strittmatter, S. M. (2008). Axonal growth therapeutics: regeneration or sprouting or plasticity? *Trends. Neurosci.* **31**, 215-220.

De Ryck, M., Van Reempts, J., Duytschaever, H., Van Deuren, B. and Clincke, G. (1992). Neocortical localization of tactile/proprioceptive limb placing reactions in the rat. *Brain Res.* **573**, 44-60.

Dergham, P., Ellezam, B., Essagian, C., Avedissian, H., Lubell, W. D. and McKerracher, L. (2002). Rho signaling pathway targeted to promote spinal cord repair. *J. Neurosci.* **22**, 6570-6577.

Dubreuil, C. I., Winton, M. J. and McKerracher, L. (2003). Rho activation patterns after spinal cord injury and the role of activated Rho in apoptosis in the central nervous system. *J. Cell Biol.* **162**, 233-243.

Fischer, D., Petkova, V., Thanos, S. and Benowitz, L. I. (2004). Switching mature retinal ganglion cells to a robust growth state in vivo: gene expression and synergy with RhoA inactivation. *J. Neurosci.* **24**, 8726-8740.

Fournier, A. E., Takizawa, B. T. and Strittmatter, S. M. (2003). Rho kinase inhibition enhances axonal regeneration in the injured CNS. *J. Neurosci.* **23**, 1416-1423.

Fuller, M. L., DeChant, A. K., Rothstein, B., Caprariello, A., Wang, R., Hall, A. K. and Miller, R. H. (2007). Bone morphogenetic proteins promote gliosis in demyelinating spinal cord lesions. *Ann. Neurol.* **62**, 288-300.

Guntinas-Lichius, O., Irintchev, A., Streppel, M., Lenzen, M., Grosheva, M., Wewetzer, K., Neiss, W. F. and Angelov, D. N. (2005). Factors limiting motor recovery after facial nerve transection in the rat: combined structural and functional analyses. *Eur. J. Neurosci.* **21**, 391-402.

Hoffmann, A., Hofmann, F., Just, I., Lehnardt, S., Hanisch, U. K., Brück, W., Kettenmann, H., Ahnert-Hilger, G. and Höltje, M. (2008). Inhibition of Rho-dependent pathways by Clostridium botulinum C3 protein induces a proinflammatory profile in microglia. *Glia* **56**, 1162-1175.

Höltje, M., Hoffmann, A., Hofmann, F., Mucke, C., Grosse, G., Van Rooijen, N., Kettenmann, H., Just, I. and Ahnert-Hilger, G. (2005). Role of Rho GTPase in astrocyte morphology and migratory response during in vitro wound healing. *J. Neurochem.* **95**, 1237-1248.

Höltje, M., Hofmann, F., Lux, R., Veh, R. W., Just, I. and Ahnert-Hilger, G. (2008). Glutamate uptake and release by astrocytes are enhanced by Clostridium botulinum C3 protein. *J. Biol. Chem.* **283**, 9289-9299.

Höltje, M., Djalali, S., Hofmann, F., Münster-Wandowski, A., Hendrix, S., Boato, F., Dreger, S. C., Grosse, G., Henneberger, C., Grantyn, R. et al. (2009). A 29-amino acid fragment of Clostridium botulinum C3 protein enhances neuronal outgrowth, connectivity, and reinnervation. *FASEB J.* **23**, 1115-1126.

Iwata, Y., Ozaki, N., Hirata, H., Sugiura, Y., Horii, E., Nakao, E., Tatebe, M., Yazaki, N., Hattori, T., Majima, M. and Ishiguro, N. (2006). Fibroblast growth factor-2 enhances functional recovery of reinnervated muscle. *Muscle Nerve* **34**, 623-630.

Jacobs, B. L., Martín-Cora, F. J. and Fornal, C. A. (2002). Activity of medullary serotonergic neurons in freely moving animals. *Brain Res. Brain. Res. Rev.* **40**, 45-52.

Jain, A., Brady-Kalnay, S. M. and Bellamkonda, R. V. (2004). Modulation of Rho GTPase activity alleviates chondroitin sulfate proteoglycan-dependent inhibition of neurite extension. *J. Neurosci. Res.* **77**, 299-307.

Jin, Z. and Strittmatter, S. M. (1997). Rac1 mediates collapsin-1-induced growth cone collapse. *J. Neurosci*. **17**, 6256-6263.

Kim, J. E., Liu, B. P., Park, J. H. and Strittmatter, S. M. (2004). Nogo-66 receptor prevents raphespinal and rubrospinal axon regeneration and limits functional recovery from spinal cord injury. *Neuron* **44**, 439-451.

Lehmann, M., Fournier, A., Selles-Navarro, I., Dergham, P., Sebok, A., Leclerc, N., Tigyi, G. and McKerracher, L. (1999). Inactivation of Rho signaling pathway promotes CNS axon regeneration. *J. Neurosci.* **19**, 7537-7547.

Lord-Fontaine, S., Yang, F., Diep, Q., Dergham, P., Munzer, S., Tremblay, P. and McKerracher, L. (2008). Local inhibition of Rho signaling by cell-permeable recombinant protein BA-210 prevents secondary damage and promotes functional recovery following acute spinal cord injury. *J. Neurotrauma* **25**, 1309-1322.

Metz, G. A. and Whishaw, I. Q. (2002). Cortical and subcortical lesions impair skilled walking in the ladder rung walking test: a new task to evaluate fore- and hindlimb stepping, placing, and co-ordination. *J. Neurosci. Methods* **115**, 169-179.

Müllner, A., Gonzenbach, R. R., Weinmann, O., Schnell, L., Liebscher, T. and Schwab, M. E. (2008). Lamina-specific restoration of serotonergic projections after Nogo-A antibody treatment of spinal cord injury in rats. *Eur. J. Neurosci*. **27**, 326-333.

Niederöst, B., Oertle, T., Fritsche, J., McKinney, R. A. and Bandtlow, C. E. (2002). Nogo-A and myelin-associated glycoprotein mediate neurite growth inhibition by antagonistic regulation of RhoA and Rac1. *J. Neurosci*. **22**, 10368-10376.

Pautsch, A., Vogelsgesang, M., Tränkle, J., Herrmann, C. and Aktories, K. (2005). Crystal structure of the C3bot-RalA complex reveals a novel type of action of a bacterial exoenzyme. *EMBO J.* **24**, 3670-3680.

Rajaofetra, N., Poulat, P., Marlier, L., Sandillon, F., Drian, M. J., König, N., Famose, F., Verschuere, B,. Gouy, D., Geffard, M. and Privat, A. (1992). Transplantation of embryonic serotoninimmunoreactive neurons into the transected spinal cord of adult monkey (Macaca fascicularis). *Brain Res*. **572**, 329-334.

Ruff, R. L., McKerracher, L., Selzer, M. E. (2008). Repair and neurorehabilitation strategies for spinal cord injury. *Ann. NY Acad. Sci.* **1142**, 1-20.

Schweigreiter, R., Walmsley, A. R., Niederöst, B., Zimmermann, D. R., Oertle, T., Casademunt, E., Frentzel, S., Dechant, G., Mir, A. and Bandtlow, C. E. (2004). Versican V2 and the central inhibitory domain of Nogo-A inhibit neurite growth via p75NTR/NgR-independent pathways that converge at RhoA. *Mol. Cell. Neurosci.* **27**, 163-174.

Sekhon, L. H and Fehlings, M. G. (2001). Epidemiology, demographics, and pathophysiology of acute spinal cord injury. *Spine* **26**, 2-12.

Sheng, H., Wang, H., Homi, H. M., Spasojevic, I., Batinic-Haberle, I., Pearlstein, R. D. and Warner, D. S. (2004). A no-laminectomy spinal cord compression injury model in mice. *J. Neurotrauma* **21**, 595-603.

Sicotte, M., Tsatas, O., Jeong, S. Y., Cai, C. Q., He, Z. and David, S. (2003). Immunization with myelin or recombinant Nogo-66/MAG in alum promotes axon regeneration and sprouting after corticospinal tract lesions in the spinal cord. *Mol. Cell. Neurosci.* **23**, 251-263.

Sieber-Blum, M., Schnell, L., Grim, M., Hu, Y. F., Schneider, R. and Schwab, M. E. (2006). Characterization of epidermal neural crest stem cell (EPI-NCSC) grafts in the lesioned spinal cord. *Mol. Cell. Neurosci.* **32**, 67-81.

Simonen, M., Pedersen, V., Weinmann, O., Schnell, L., Buss, A., Ledermann, B., Christ, F., Sansig, G., van der Putten, H. and Schwab, M. E. (2003). Systemic deletion of the myelin-associated outgrowth inhibitor Nogo-A improves regenerative and plastic responses after spinal cord injury. *Neuron* **38**, 201-211.

Skagerberg, G. and Björklund, A. (1985). Topographic principles in the spinal projections of serotonergic and non-serotonergic brainstem neurons in the rat. *Neuroscience* **15**, 445-480.

Steward, O., Zheng, B. and Tessier-Lavigne, M. (2003). False resurrections: distinguishing regenerated from spared axons in the injured central nervous system. *J. Comp. Neurol*. **459**, 1-8.

Vogelsgesang, M., Pautsch, A. and Aktories, K. (2007). C3 exoenzymes, novel insights into structure and action of Rho-ADP-ribosylating toxins. *Naunyn Schmiedebergs Arch. Pharmacol.* **5-6**, 347-360.

Wang, X., Budel, S., Baughman, K., Gould, G., Song, K. H. and Strittmatter, S. M. (2009). Ibuprofen enhances recovery from spinal cord injury by limiting tissue loss and stimulating axonal growth. *J. Neurotrauma* **26**, 81-95.

Wilde, C., Barth, H., Sehr, P., Han, L., Schmidt, M., Just, I. and Aktories, K. (2002). Interaction of the Rho-ADP-ribosylating C3 exoenzyme with RalA. *J. Biol. Chem.* **277**, 14771-14776..

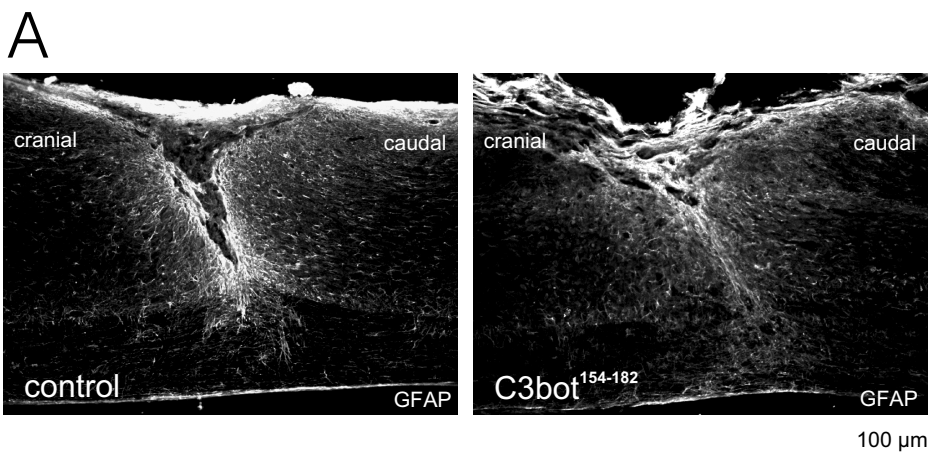
A
cranial
caudal
control
GFAP
cranial
caudal
C3bot154-182
GFAP
100 µm
B
lesion size
GFAP
mm²
0.35
0.3
0.25
0.2
0.15
0.1
0.05
0
control
C3bot154-182
C
gliosis
cranial
caudal
GFAP expression [AU]
30
25
20
15
10
5
0
control
C3bot154-182
6 5 4 3 2 1 0 -1 -2 -3 -4 -5 -6
distance to lesion center (µm x 100)

A

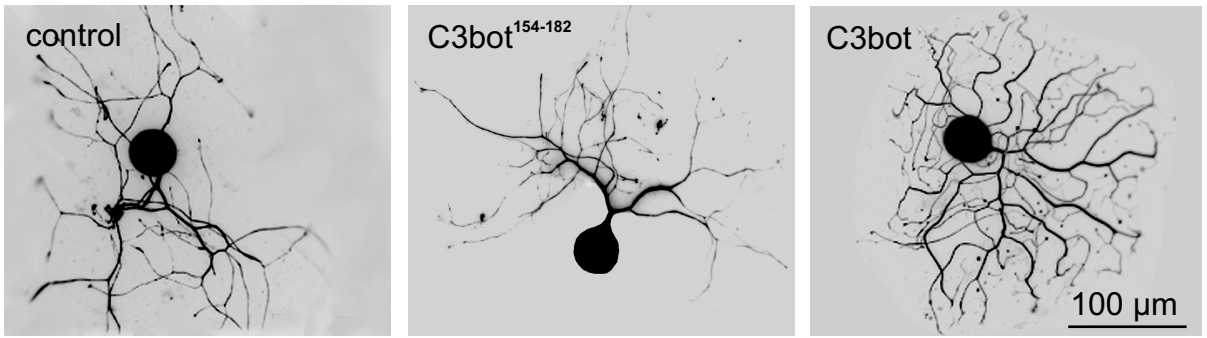
control
C3bot154-182
C3bot
100 µm

B

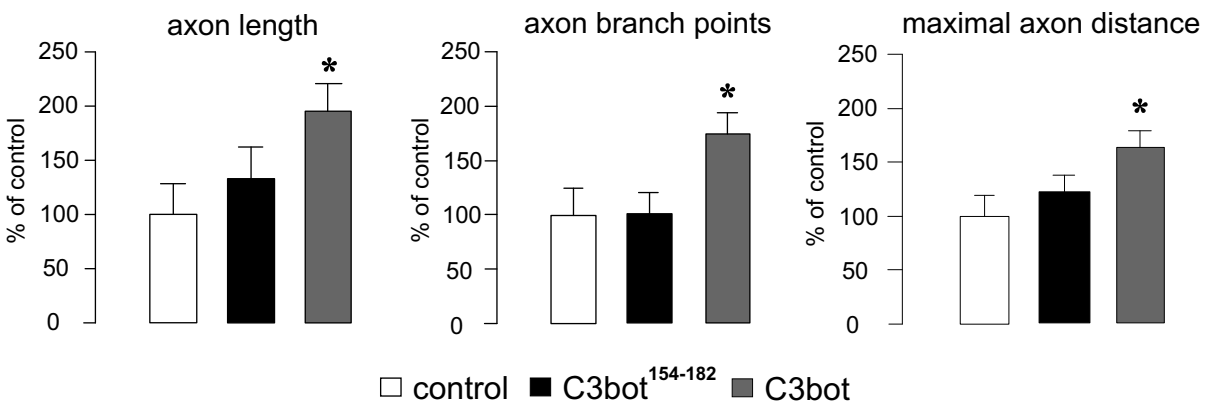
axon length
axon branch points
maximal axon distance
% of control
250
200
150
100
50
0
*
control
C3bot154-182
C3bot